Disulfide bond effects on protein stability: Designed variants of *Cucurbita maxima* trypsin inhibitor-V

MARIA ZAVODSZKY,[1] CHAO-WEI CHEN,[2] JENQ-KUEN HUANG,[2]
MICHAL ZOLKIEWSKI,[1] LISA WEN,[2] AND RAMASWAMY KRISHNAMOORTHI[1]

[1]Department of Biochemistry, Kansas State University, Manhattan, Kansas 66506, USA
[2]Department of Chemistry, Western Illinois University, Macomb, Illinois 61455, USA

(RECEIVED June 28, 2000; FINAL REVISION October 12, 2000; ACCEPTED November 1, 2000)

Abstract

Attempts to increase protein stability by insertion of novel disulfide bonds have not always been successful. According to the two current models, cross-links enhance stability mainly through denatured state effects. We have investigated the effects of removal and addition of disulfide cross-links, protein flexibility in the vicinity of a cross-link, and disulfide loop size on the stability of *Cucurbita maxima* trypsin inhibitor-V (CMTI-V; 7 kD) by differential scanning calorimetry. CMTI-V offers the advantage of a large, flexible, and solvent-exposed loop not involved in extensive intra-molecular interactions. We have uncovered a negative correlation between retention time in hydrophobic column chromatography, a measure of protein hydrophobicity, and melting temperature (T_m), an indicator of native state stabilization, for CMTI-V and its variants. In conjunction with the complete set of thermodynamic parameters of denaturation, this has led to the following deductions: (1) In the less stable, disulfide-removed C3S/C48S ($\Delta\Delta G_d^{50°C} = -4$ kcal/mole; $\Delta T_m = -22°C$), the native state is destabilized more than the denatured state; this also applies to the less-stable CMTI-V* ($\Delta\Delta G_d^{50°C} = -3$ kcal/mole; $\Delta T_m = -11°C$), in which the disulfide-containing loop is opened by specific hydrolysis of the Lys^{44}-Asp^{45} peptide bond; (2) In the less stable, disulfide-inserted E38C/W54C ($\Delta\Delta G_d^{50°C} = -1$ kcal/mole; $\Delta T_m = +2°C$), the denatured state is more stabilized than the native state; and (3) In the more stable, disulfide-engineered V42C/R52C ($\Delta\Delta G_d^{50°C} = +1$ kcal/mole; $\Delta T_m = +17°C$), the native state is more stabilized than the denatured state. These results show that a cross-link stabilizes *both* native and denatured states, and differential stabilization of the two states causes either loss or gain in protein stability. Removal of hydrogen bonds in the same flexible region of CMTI-V resulted in less destabilization despite larger changes in the enthalpy and entropy of denaturation. The effect of a cross-link on the denatured state of CMTI-V was estimated directly by means of a four-state thermodynamic cycle consisting of native and denatured states of CMTI-V and CMTI-V*. Overall, the results show that an enthalpy-entropy compensation accompanies disulfide bond effects and protein stabilization is profoundly modulated by altered hydrophobicity of both native and denatured states, altered flexibility near the cross-link, and residual structure in the denatured state.

Keywords: Disulfide-bond; cross-link; protein stability; differential scanning calorimetry; denaturation; folding

Supplemental material: See www.proteinscience.org.

The conformational stability of a protein is important to its function. Certain diseases such as Alzheimer's, prion, and cystic fibrosis, are associated with misfolded, unfolded, or aggregated proteins (Kelly 1996; Harper and Lansbury, Jr. 1997; Horwich and Weissman 1997, Qu et al. 1997). Much has been characterized regarding contributions to protein stability of hydrogen bonds, ion-pairs, van der Waals, and hydrophobic interactions (Dill 1990; Nosoh and Sekiguchi 1991; Richards and Lim 1994; Vogt et al. 1997). The native

Reprint request to: Ramaswamy Krishnamoorthi, Department of Biochemistry, 103 Willard Hall, Kansas State University, Manhattan, Kansas 66506, USA; e-mail: krish@ksu.edu; fax: 785-532-7278.

Abbreviations: CMTI-V, *Cucurbita maxima* trypsin inhibitor-V; DSC, differential scanning calorimetry; ΔC_p, heat capacity change; T_m, melting temperature; CD, circular dichroism; HPLC, high pressure liquid chromatography; SDS-PAGE, sodium dodecylsulfate polyacrylamide gel electrophoresis; DTNB, 5,5′-dithiobis(2-nitrobenzoic acid).

Article and publication are at www.proteinscience.org/cgi/doi/10.1110/ps.26801.

or folded state of a protein is only 5 to 10 kcal/mole more stable than its denatured or unfolded state (Creighton 1993). The stability of proteins is substantially increased by naturally occurring disulfide cross-links. A disulfide bond can contribute as much as 5 to 6 kcal/mole to the stability of the folded protein at optimal temperature (Matsumura and Matthews 1991; Betz 1993; Darby and Creighton 1995). Thus, insertion of a novel disulfide bond into a protein is an attractive strategy to improve its stability. However, attempts to improve protein stability by introducing artificial disulfide bridges have yielded limited success. In some cases, introduction of a disulfide bond has led to protein destabilization (Betz 1993; Johnson et al. 1997).

According to the classical chain-entropy model (Flory 1956; Poland and Scheraga 1965; Lin et al. 1984; Pace et al. 1988), increased stability results primarily from decreased entropy of the denatured state. Destabilization, as measured by changes in chemical or thermal denaturation free energies, $\Delta\Delta G_d$, caused by removal of naturally occurring disulfide bonds has been correlated to the changes in configurational entropy of the denatured state:

$$\Delta\Delta G_d = -T\Delta\Delta S_d = -T[-2.1 - (3/2)\ R \ln n] \qquad (1)$$

in which R is the universal gas constant and n is the loop size—the number of residues enclosed by the disulfide link (Pace et al. 1988). The average size of naturally occurring loops is 15 (Thornton 1981).

The Doig and Williams model (1991), developed from an analysis of denaturation data of several proteins, holds the view that reduced protein-solvent interactions in the denatured state of the cross-linked protein lead to entropic and enthalpic increases, and a net increase in the denaturation free energy is caused by a dominant increase in the denaturation enthalpy. Thus, according to both models, the disulfide bond enhances stability by primarily acting on the unfolded state of the protein.

Despite many studies involving removal of natural disulfide links (Schwartz et al. 1987; Pace et al. 1988; Eigenbrot et al. 1990; Cooper et al. 1992; Ikeguchi et al. 1992; Kuroki et al. 1992; Vogl et al. 1995; Bonander et al. 2000; Klink et al. 2000) and insertion of novel ones (Sauer et al. 1986; Wells and Powers 1986; Pantoliano et al. 1987; Villafranca et al. 1987; Pjura et al. 1990; Takagi et al. 1990; Matsumura and Matthews 1991; Clarke and Fersht 1993; Clarke et al. 1995; Hinck et al. 1996; Johnson et al. 1997; Futami et al. 2000), including those made by chemical modification (Goldenberg and Creighton 1983; Lin et al. 1984; Ueda et al. 1985), our understanding of the mechanism of stabilization of proteins by cross-links is far from complete. Loop length alone does not fully account for observed changes in denaturation free energy or entropy (Zhang et al. 1994; Vogl et al. 1995; Balbach et al. 1998) Disulfide mutants show decreased as well as increased stabilities, and their denaturation thermodynamic parameters do not support the Doig and Williams model (Matsumura and Matthews 1991; Johnson et al. 1997).

Steric and electrostatic effects of the amino acid sidechains that replace the disulfide bond are believed to influence protein stability (Vogl et al. 1995; Balbach et al. 1998). Theoretical studies indicate that destabilization by a cross-link can occur through reduction of configurational entropy of the folded state (Tidor and Karplus 1993). Strain in disulfide dihedral angle(s) has also been implicated in loss of stability (Katz and Kossiakoff 1986; Matsumura and Matthews 1991). In contrast, X-ray crystallographic studies of some disulfide mutants show that stability is not affected by the conformation of the disulfide bridge (Clarke et al. 1995).

It is, therefore, useful to identify and evaluate quantitatively different factors by which a cross-link alters stability of the folded and denatured states of a protein. We have adopted a simple strategy of comparing and correlating differences in thermodynamics of denaturation with differences in physical properties for mutants of a protein, in which a cross-link is inserted into or removed from the same flexible region, but at different sites. We have used for this purpose *Cucurbita maxima* trypsin inhibitor-V (CMTI-V), a small, globular protein of 68 residues, including a Cys^3-Cys^{48} link. We have previously determined the three-dimensional solution structures of both natural and wild-type recombinant proteins (Fig. 1; Cai et al. 1995a; Liu et al. 1996). CMTI-V has a large, flexible, and solvent-exposed loop, whose residues (37–48) are not involved in extensive interactions with others. Two hydrogen bonds—one between Thr^{43} and Arg^{52}, the other between Asp^{45} and Arg^{50}—anchor the loop to the protein scaffold and, hence, provide additional avenues for assessing the thermodynamic effects of cross-link removal. The architecture of CMTI-V has permitted us to prepare disulfide mutants with different loop sizes and a cleaved form of the protein, CMTI-V*, by specific hydrolysis of the Lys^{44}-Asp^{45} peptide bond (Krishnamoorthi et al. 1990). CMTI-V* has both of its fragments connected by the Cys^3-Cys^{48} bridge and, thus, represents an unlinked version of the disulfide loop. This has facilitated a direct determination of the entropy effect of a cross-link on the denatured state of CMTI-V by means of a four-state thermodynamic cycle involving native and denatured forms of CMTI-V and CMTI-V*.

Herein we present results that, besides proving the inadequacy of either of the two models, show that hydrophobicity of a folded protein is significantly changed by a disulfide cross-link depending on its location, and such a change is negatively correlated with folded state stabilization. Protein flexibility in the vicinity of a natural disulfide bridge and context-dependent residual structure in the denatured state because of an engineered cross-link also influence protein stability.

Results

Variants

Thermal denaturation studies of wild-type CMTI-V and the following mutants were performed by differential scanning calorimetry (DSC): C3S/C48S, E38C/W54C, V42C/R52C, R50A, R50K, R52A, R52Q, T43A, and P4G (see Fig. 1). In the C3S/C48S double mutant, the natural disulfide bond, located at one end of the trypsin-binding loop of the protein, is removed. The E38C/W54C double mutant has an additional disulfide bond introduced at the other end of the binding loop. In V42C/R52C, the second disulfide bond is located in the middle of the protease-binding loop. The double mutants allowed us to determine the effect of the disulfide loop size on stability. CMTI-V*, in which the loop formed by the Cys^{3}-Cys^{48} link is opened at the Lys^{44}-Asp^{45} peptide bond (Cai et al. 1995b), was used in a four-state thermodynamic cycle to evaluate the denatured state effects of a cross-link, as described later.

Single mutants—R50A, R50K, R52A, R52Q, and T43A—were constructed to characterize the effect of removal of the Arg^{50}..Thr^{43} and Arg^{52}..Asp^{45} hydrogen bonds that cross-link the flexible loop to the core (Cai et al. 1995a). The P4G mutant was designed to evaluate the consequences of flexibility conferred on a site adjacent to the Cys^{3}-Cys^{48} bridge.

DSC endotherms of CMTI-V and the variants are shown in Figure 2. The unfolding reactions of CMTI-V and the mutants were highly reversible in the pH range 2.0 to 3.5 (Fig. S-1 in Electronic Supplemental Material). Reversibility of DSC scans of CMTI-V* indicated that the native disulfide bond remained intact even when the protein was heated above 100°C. The stability changes caused by the mutations cover a wide range: there is an almost 40°C difference between the lowest T_m measured for C3S/C48S, the disulfide-deficient mutant, and the highest T_m observed for V42C/R52C, which has an extra disulfide bond relative to CMTI-V. Thermodynamic data of denaturation of CMTI-V and its variants at pH 2.5 are presented in Table 1.

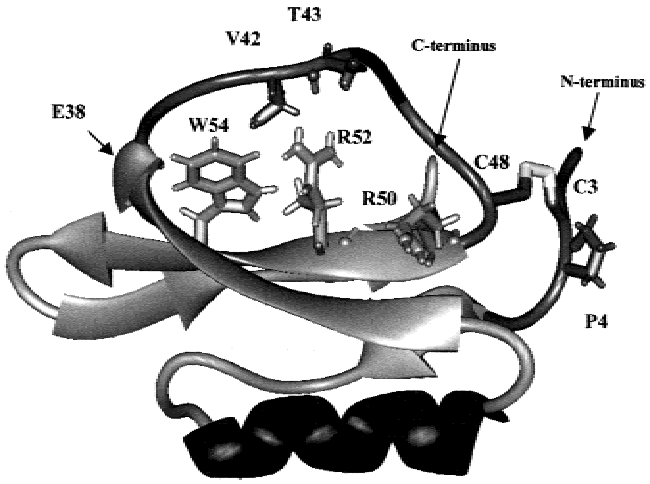

Fig. 1. NMR solution structure of CMTI-V (Cai et al. 1995a; Liu et al. 1996) showing the residues replaced in the various mutants studied. The protein contains a rigid scaffold and a flexible loop region. The scaffold consists of an α-helix and three β-sheets (two antiparallel and one parallel) connected by the flexible loop and four turns.

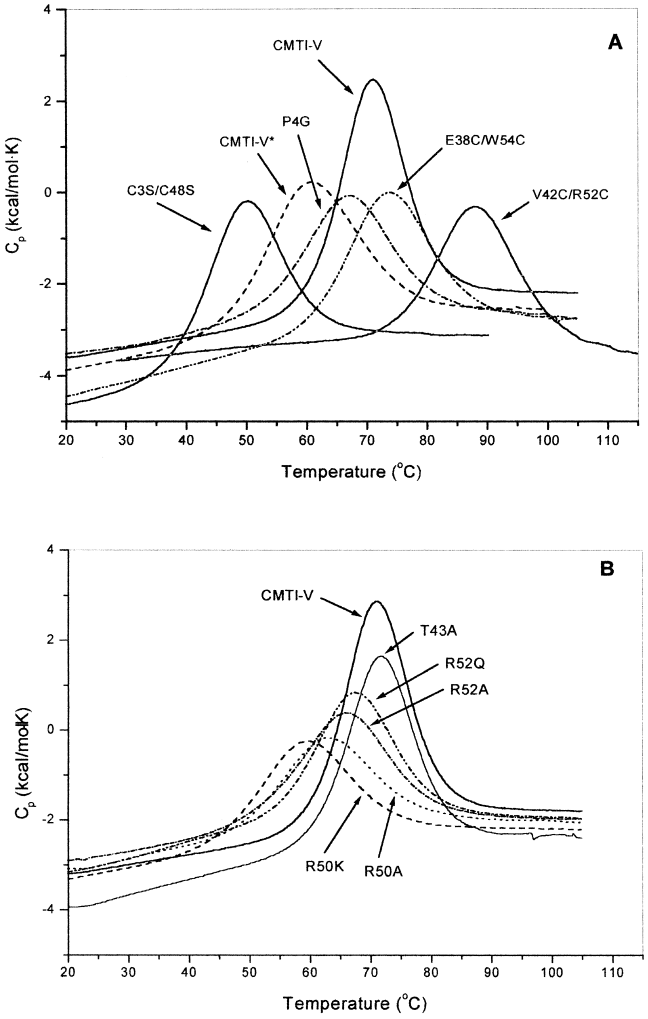

Fig. 2. Differential scanning calorimetry endotherms of CMTI-V and mutants at pH 2.5 showing a wide range of melting temperatures. Variants include: (*A*) Disulfide-deletion and -insertion mutants and (*B*) hydrogen-bond mutants

Effects on T_m and ΔC_p

Removal of the disulfide bridge in C3S/C48S causes the largest decrease in T_m (22°C) among the mutants studied. The unlinked CMTI-V* has a 11°C lower T_m, relative to CMTI-V. Both V42C/R52C and E38C/W54C, each having an extra disulfide bond, show elevated T_m. The 38–54 disulfide bond produces only a 3°C increase, whereas the 42–52 cross-link increases T_m by 17°C. Removal of a hy-

Table 1. *Thermodynamic parameters of thermal denaturation of CMTI-V and mutants at pH 2.5*

Protein	T_m (°C)[a]	ΔH_m (kcal/mol)[b]	ΔS_m (cal/mol · K)	ΔC_p (kcal/mol · K)[c]	$\Delta\Delta C_p$ (mut-wt) (kcal/mol · K)
CMTI-V	70.9	64	185	0.42	—
CMTI-V*	60.4	53	158	0.46	0.04
C3S/C48S	49.2	50	156	0.59	0.17
E38C/W54C	73.6	43	125	0.33	–0.09
V42C/R52C	87.8	47	129	0.15	–0.27
R50A	62.6	31	93	0.13	–0.29
R50K	59.2	35	107	0.23	–0.19
R52A	65.7	43	128	0.24	–0.18
R52Q	67.5	42	124	0.27	–0.15
P4G	66.7	45	132	0.56	0.14
T43A	71.7	58	167	0.34	–0.08

[a] Estimated error ± 0.1°C.
[b] Estimated error ± 1 kcal/mol.
[c] Estimated error ± 10%.

drogen bond from the same binding-loop region of CMTI-V (see Fig. 1) shows position-dependent effects: R50A and R50K unfold at ~10°C lower than does CMTI-V, whereas the T_m of R52A and R52Q is only ~5°C lower. Surprisingly, substitution of Pro^4 in the N-terminal part is more destabilizing than that of Thr^{43} in the middle of the long flexible loop. The side-chain of Thr^{43} is implicated in the hydrogen bond formed by Arg^{52} (Cai et al. 1995a). However, T43A has an almost unchanged T_m. This indicates that Arg^{52} probably makes a hydrogen bond with the oxygen atom of Ala^{43}.

Denaturation causes a very small change in heat capacity (ΔC_p) of 0.42 kcal/mole · K for CMTI-V (Table 1). CMTI-V*, which has the loop opened at the Lys^{44}-Asp^{45} site, has an almost unchanged ΔC_p. Only P4G and C3S/C48S show raised ΔC_p values (positive $\Delta\Delta C_p$). All the other mutants show decreases in ΔC_p (negative $\Delta\Delta C_p$).

Increased hydrophobicity/decreased hydrophilicity of the native state or increased hydrophilicity/decreased hydrophobicity of the denatured state can account for decreased ΔC_p (negative $\Delta\Delta C_p$ in Table 1; Privalov and Makhatadze 1992). Increased hydrophilicity or reduced hydrophobicity of a protein is expected to stabilize more its native state and reduce its retention time on a C_{18}-hydrophobic column, as the hydrophobicity of the eluent mixture (acetonitrile and water) is gradually increased. Changes in the native state stabilization of a protein are most likely reflected by changes in its T_m (Matsumura and Matthews 1991). Figure 3 illustrates a plot of T_m versus retention time in reverse-phase high-pressure liquid chromatography (HPLC) determined for CMTI-V and its mutants. Indeed, a negative correlation is observed between the two and, thus, provides an insight into the nature of native state effects of a cross-link.

Effects on ΔH_d, ΔS_d, and ΔG_d

Calculated thermodynamic parameters of denaturation at 50°C of CMTI-V and its variants are collected in Table 2. At this temperature, which is close to the melting temperatures observed, almost all of the mutants exist in the folded state, and the effect of error in ΔC_p on the computed thermodynamic quantities is minimized (see Materials and Methods). For every mutant, except C3S/C48S, both ΔH_d and ΔS_d are decreased, and the fine balance between these two quantities determines whether the mutant is stabilized or destabilized. The 4 kcal/mole destabilization experienced by C3S/C48S appears to be purely enthalpic in origin. CMTI-V* shows slightly decreased ΔH_d and ΔS_d with a net destabilization of 3 kcal/mole. The disulfide bond engineered in V42C/R52C increases stability by 1 kcal/mole and T_m by 17°C. In contrast, the 38–54 cross-link introduced in E38C/W54C *destabilizes* the protein by 1 kcal/mole and raises its T_m by 3°C. Figure 4 illustrates the temperature dependence of ΔG_d for CMTI-V and some of the mutants

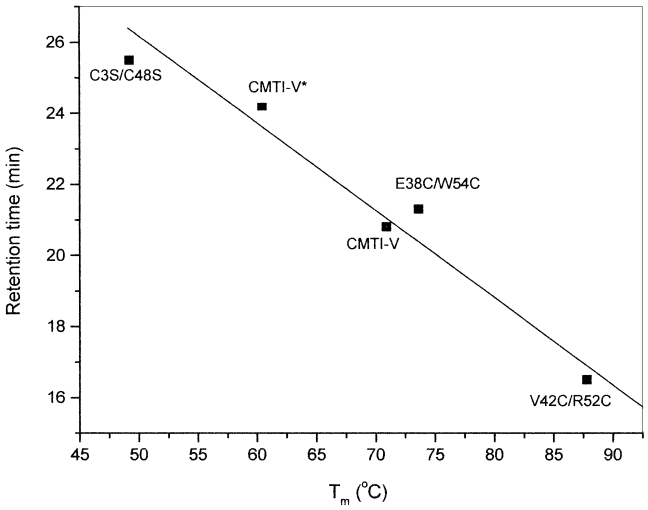

Fig. 3. Plot of high-pressure liquid chromatography retention times versus melting temperatures for CMTI-V and mutants. The line drawn represents the least-squares fit to the experimental data ($r^2 = 0.96$).

studied. Interestingly, E38C/W54C is predicted to become more stable than the wild-type protein only at temperatures higher than ~60°C.

The free energy changes determined for the removal of hydrogen bonds at 50°C are −2 kcal/mole for the R52 mutants and−3 kcal/mole for the R50 mutants (Table 2), in agreement with the range of values (1.5–4 kcal/mole) associated with exposed hydrogen bonds (Byrne et al. 1995; Takano et al. 1999). The ΔH_d and $T\Delta S_d$ values of these mutants are decreased by 15 to 25 kcal/mole and 13 to 22 kcal/mole, respectively. Removal of the R50 hydrogen bond results in a larger decrease (1.5 times) than that caused by the R52 hydrogen bond. However, T43A is less destabilized than R52A with smaller decreases in ΔH_d and ΔS_d. This is consistent with the proposed hydrogen-bonding interaction between Arg^{52} and the oxygen atom of Ala^{43}. P4G is destabilized by 2 kcal/mole, with decreases in ΔH_d and ΔS_d similar to those of hydrogen-bond mutants (Table 2).

Circular dichroism spectra of mutants

The effects of mutations on protein structure were examined by circular dichroism (CD) spectroscopy. The CD spectra of the single mutants are similar to that of the wild-type protein either at 25°C or at 85°C. The CD spectra of the double mutants at 25°C (Fig. 5A) also resemble that of the wild-type protein—typical of those composed of mainly β-sheets, turns, and a small percentage of α-helix. These spectra have the same overall shape, with relatively small differences in the 220–240 nm region. Similarity in the overall folding of the mutants is further confirmed by the fact that they all retain their ability to inhibit trypsin, albeit by different extents (Fig. S-2 in Electronic Supplemental Material). The CD spectra of CMTI-V and the mutants at 85°C are not significantly different from one another (Fig. 5B). However, the shape of these is different from the typi-

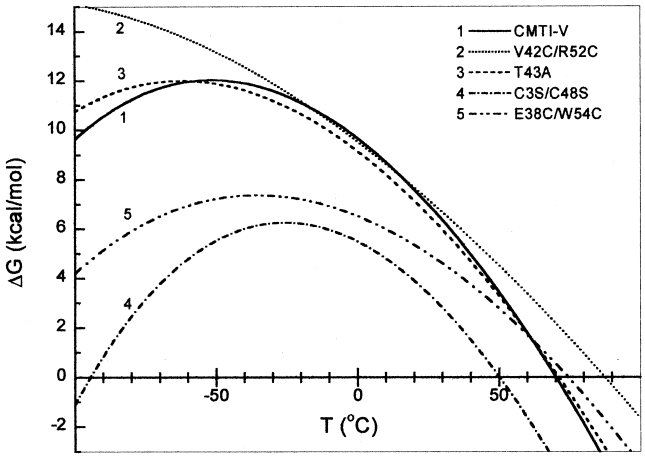

Fig. 4. Temperature dependence of free energy of denaturation for CMTI-V and mutants at pH 2.5.

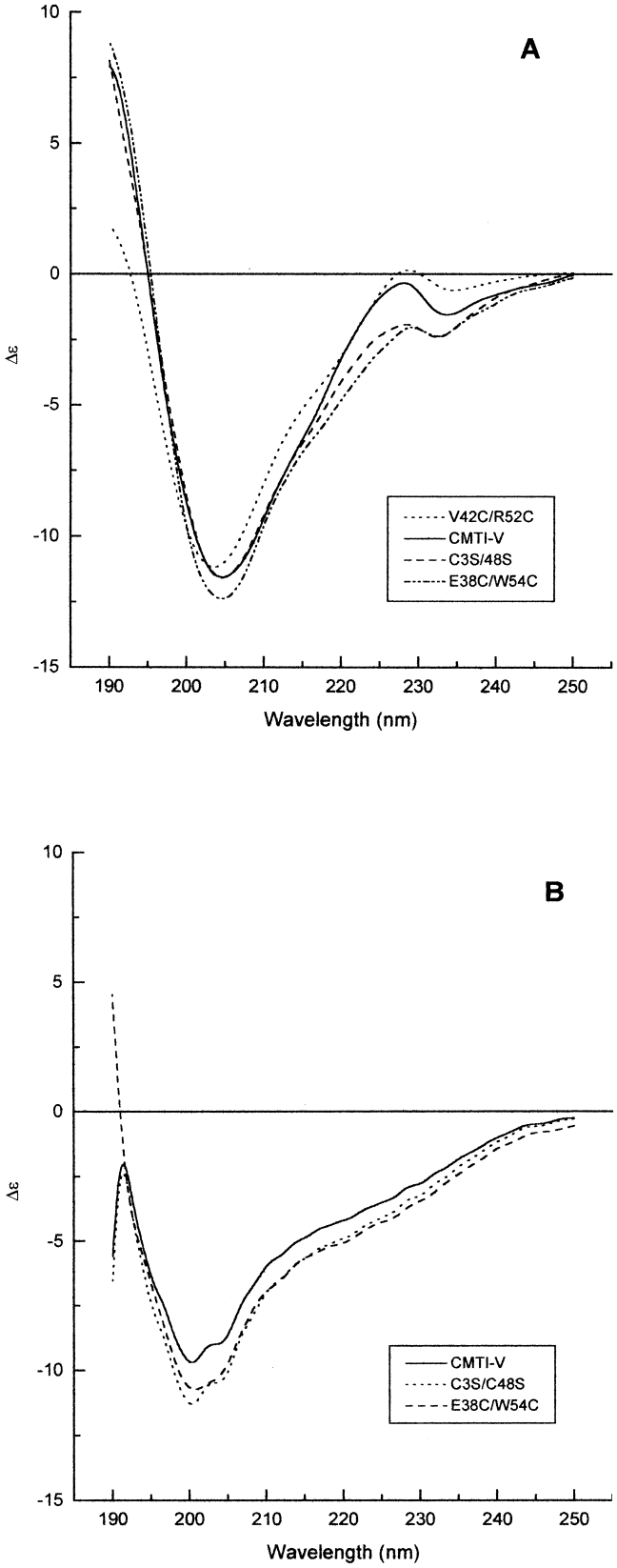

Fig. 5. CD spectra of CMTI-V and variants at pH 2.5: (*A*) at 25°C and (*B*) at 85°C.

Table 2. *Calculated thermodynamic parameters (in kcal/mol) of denaturation of CMTI-V and mutants at 50°C*

Protein	$\Delta H_d^{50°C}$	$\Delta\Delta H_d^{50°C}$ (mut-wt)	$T\Delta S_d^{50°C}$	$T\Delta\Delta S_d^{50°C}$ (mut-wt)	$\Delta G_d^{50°C}$	$\Delta\Delta G_d^{50°C}$ (mut-wt)
CMTI-V	55	—	51	—	4	—
CMTI-V*	48	−7	47	−4	1	−3
C3S/C48S	51	−4	51	0	0	−4
E38C/W54C	36	−19	33	−18	3	−1
V42C/R52C	41	−14	36	−15	5	1
R50A	30	−25	29	−22	1	−3
R50K	33	−22	32	−19	1	−3
R52A	40	−15	38	−13	2	−2
R52Q	38	−17	36	−15	2	−2
P4G	35	−20	33	−18	2	−2
T43A	50	−5	47	−4	3	−1

cal spectrum of a random coil in the 210–240 nm region (Woody 1995). This indicates the presence of some residual structure in the denatured state. The denatured proteins show a red-shifted minimum and differences in the 210–240 nm region (Fig. 5B), consistent with an increase in the random coil content compared to the native state. A CD spectrum of the completely unfolded V42C/R52C could not be obtained, as the temperature of the spectropolarimeter could not be increased above 85°C.

Discussion

Disulfide-deficient and unlinked variants

The chain-entropy model (Pace et al. 1988) predicts a destabilization of 4.1 kcal/mole at 25°C and 4.4 kcal/mole at 50°C for the disulfide-deficient mutant C3S/C48S. These values are in relatively good agreement with the experimental values of 3.6 kcal/mole at 25°C (Table T-1 in Electronic Supplemental Material) and 4 kcal/mole at 50°C (Table 2). However, thermal denaturation of C3S/C48S, in which a large loop of 46 residues is opened, is surprisingly accompanied by the same entropy change as that of CMTI-V at 50°C (Table 2). The difference in ΔG_d arises solely from the decreased enthalpy change.

Even at 25°C, in which the calculations give a decrease in the entropy change (Table T-1 in Electronic Supplemental Material), the enthalpy change is almost twice as much. These results seem to agree with the Doig and Williams model (1991), which predicts a decrease in entropy change but a larger decrease in the enthalpy change and an increase in ΔC_p.

The increase in ΔC_p experienced by C3S/C48S (Table 1; positive $\Delta\Delta C_p$) is consistent with either an increase in the exposed hydrophobic surface area of the denatured state or an increase in the hydrophilicity of the folded state (Privalov and Makhatadze 1992). However, folded C3S/C48S shows increased hydrophobicity (Fig. 3). The raised ΔC_p of C3S/C48S, therefore, implies a larger enhancement of hydrophobicity of the denatured protein. The much lower T_m recorded for this mutant attests to its native state destabilization. Similar arguments are advanced for the other unlinked form, CMTI-V*. Surprisingly, it is less hydrophilic than CMTI-V (Fig. 3), although cleavage of the 44–45 peptide bond produces an additional ionic N-terminus. CMTI-V* is more stable and has a higher T_m and lower ΔC_p relative to C3S/C48S (Tables 1,2).

On the basis of the negative correlation established between hydrophobicity and native state stabilization (Fig. 3) and the thermodynamic parameters of denaturation (Tables 1,2), we construct a free energy diagram for native and denatured C3S/C48S relative to CMTI-V in Figure 6. Furthermore, thermodynamic predictions of the two models are compared with the experimental results. For C3S/C48S, destabilization of *both* native and denatured states occurs, and decreased free energy of denaturation results from a greater native state effect. This also applies to the unlinked CMTI-V*.

In comparison, deletion of a disulfide link in hen egg white lysozyme results in a decrease in ΔS_d and no change in ΔH_d (Cooper et al. 1992). In constrast, removal of a disulfide link in human lysozyme decreases ΔH_d (Kuroki et al. 1992) and increases flexibility of the native state (Inaka et al. 1991).

Disulfide-engineered mutants

Relative to the wild-type protein, V42C/R52C is 1 kcal/mole more stable and E38C/W54C is 1 kcal/mole *less* stable at 50°C (Table 2). On the basis of the structure of CMTI-V (Fig. 1), no significant difference in stability is anticipated between the two mutants. In fact, E38C/W54C would be expected to be a little more stable: it has a larger loop size

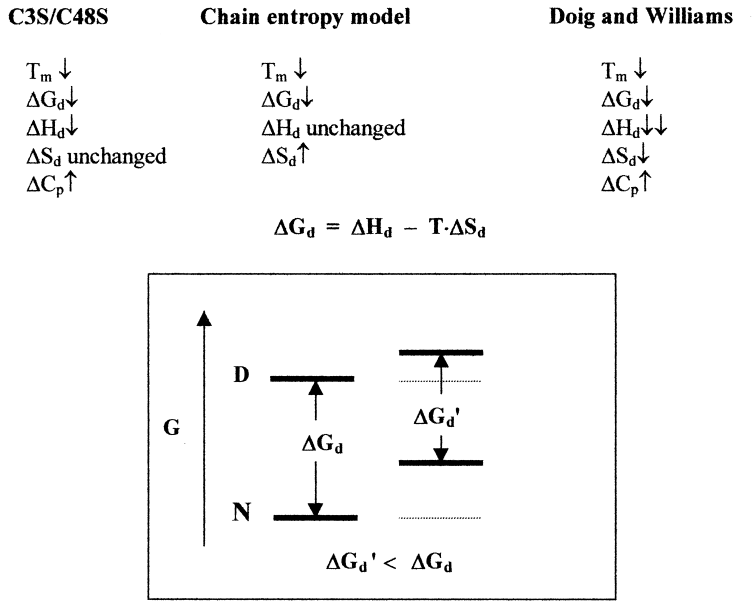

Fig. 6. Theoretical predictions of the chain-entropy model (Pace et al. 1988) and Doig and Williams (1991) versus experimental results for C3S/C48S at 50°C. The free energy diagram depicts a possible arrangement of native and denatured states of the disulfide-deficient mutant (ΔG_d') in relation to wild-type CMTI-V (ΔG_d). A similar diagram is applicable to the unlinked CMTI-V*, which shows in addition a small decrease in ΔS_d.

(17 compared with 11 in the V42C/R52C mutant) and the C_α-C_α distance between residues 38 and 54 is ~5 Å, as opposed to ~10 Å between residues 42 and 52. Formation of the 42–52 link must distort the loop conformation to some extent. Previous studies have indicated that loop length alone does not account for the observed changes in denaturation free energy or entropy of mutants in the case of T4 lysozyme (Matsumura and Matthews 1991), α-amylase inhibitor tendamistat (Vogl et al. 1995), and barnase (Johnson et al. 1997).

The increase in ΔG_d caused by the decrease in ΔS_d, according to the chain-entropy model, should be about 3 to 3.4 kcal/mole for E38C/W54C and V42C/R52C. Instead, we found that $T\Delta S_d$ decreases 5 times as much (Table 2). Likewise, both V42C/R52C and E38C/W54C show, contrary to the predictions of the Doig and Williams model (1991), *decreases* in *both* ΔH_d and ΔS_d. For E38C/W54C, the decrease in ΔH_d is slightly larger than the decrease in ΔS_d, whereas the opposite is true for V42C/R52C.

Both E38C/W54C and V42C/R52C experience decreases in ΔC_p (Table 1; negative $\Delta\Delta C_p$). This appears to be in agreement with the Doig and Williams model (1991), which attributes it to decreased unfolded state hydration.

ΔC_p of the more stable V42C/R52C is only 0.15 kcal/mole·K, compared with 0.33 kcal/mole K of the less stable E38C/W54C. Relative to the wild-type protein, E38C/W54C has similar hydrophobicity, whereas V42C/R52C is more hydrophilic (Fig. 3). The decreased ΔC_p values of these mutants (Table 1; negative $\Delta\Delta C_p$), therefore, indicate that in the denatured state both E38C/W54C and V42C/R52C are *less* hydrophobic than the wild-type protein, most likely because of the presence of residual structure in the denatured states of these mutants (Privalov et al. 1989). The CD spectra of CMTI-V and E38C/W54C at 25°C and 85°C (Fig. 5A,B) appear to support this view. We also deduce that denatured E38C/W54C is stabilized, relative to denatured V42C/R52C, by both enthalpic and entropic contributions (Table 2), likely because of the presence of more pronounced residual structure. Residual structure in the denatured state has been noted in the case of staphylococcal nuclease mutants (Shortle 1996; Wang and Shortle 1997), cross-linked cytochrome *c* (Betz and Pielak 1992; Betz et al. 1996), lysozyme (Buck et al. 1996), and barnase (Wong et al. 2000).

Using the negative correlation between hydrophobicity and T_m, as established in Figure 3, in conjunction with the thermodynamic parameters of denaturation (Tables 1,2), we generate free energy diagrams for native and denatured states of E38C/W54C and V42C/R52C in Figure 7. *Both* native and denatured states are stabilized for the two mutants. However, the denatured state is more stabilized in E38C/W54C, and the native state is more stabilized in V42C/R52C. Consequently, E38C/W54C is *less* stable and V42V/R52C is *more* stable than the wild-type protein at 50°C.

Decreased stabilities of mutants of λ-cro (Pakula and Sauer 1990), staphylococcal nuclease (Schwehm et al. 1998), and human lysozyme (Takano et al. 1998) have been

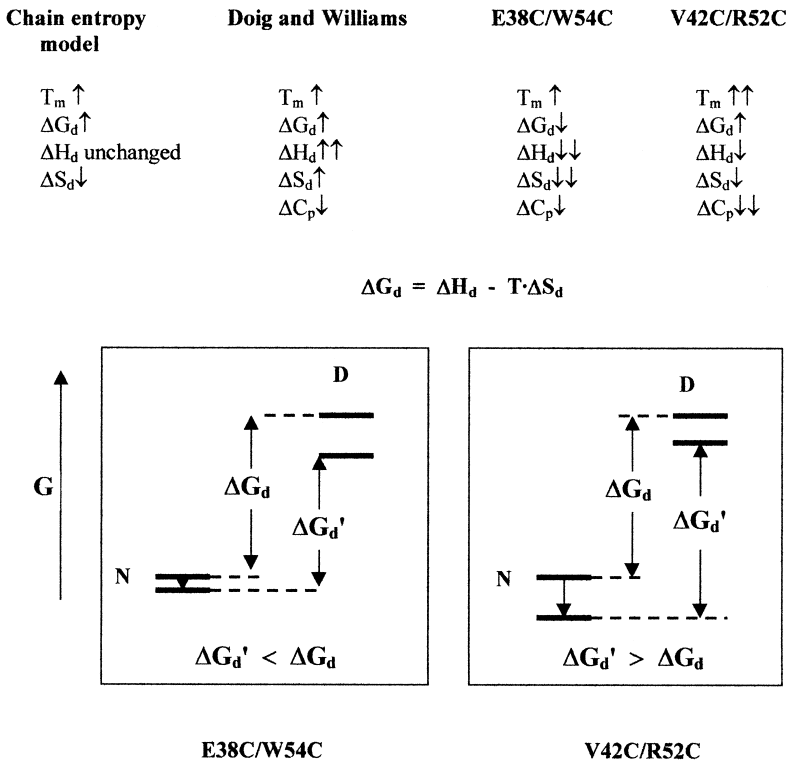

Fig. 7. Theoretical predictions of the chain-entropy model (Pace et al. 1988) and Doig and Williams (1991) *vs* experimental results for E38C/W54C and V42C/R52C. The free energy diagrams show possible arrangements of native and denatured states of the two disulfide-engineered mutants (ΔG_d'), relative to wild-type CMTI-V (ΔG_d).

attributed to increased hydrophobicity of surface residues in the native state relative to the denatured state.

In some instances, decreased stability (lower T_m) has been ascribed to strain in disulfide bond and increased stability (higher T_m) to flexibility of Cys-engineered sites (Matsumura and Matthews 1991). In contrast, X-ray crystallographic studies of disulfide mutants of barnase (Clarke et al. 1995) show that stability is not affected by the dihedral geometry of the cross-link. Theoretical calculations indicate that a cross-link can destabilize the folded state by entropic loss (Tidor and Karplus 1993), similar to unfolded state effects (Lin et al. 1984).

The present study shows that an experimental measure of hydrophobicity, along with the complete set of thermodynamic parameters of protein denaturation, can help clarify the differential effects of removal or insertion of a disulfide bond and their context-dependence on *both* folded and denatured states of a protein. This is particularly useful in view of the fact that three-dimensional structures of disulfide mutants in some cases have yielded limited insight into their varying stability (Katz and Kossiakoff 1986, 1990; Matsumura and Matthews 1991; Clarke et al. 1995; Balbach et al. 1998; Bonander et al. 2000).

Variants lacking a cross-linking hydrogen bond

Results from R50 and R52 mutants of CMTI-V (Tables 1,2) show that removal of a cross-linking hydrogen bond from the same flexible loop of CMTI-V (Fig. 1) results in destabilization, with decrease in every thermodynamic, parameter: T_m, ΔH_d, ΔS_d, ΔC_p, and ΔG_d. These results are consistent with the expectation of increased enthalpy, flexibility, or configurational entropy, and decreased stability of the folded state. The P4G mutant shows similar decreases in T_m, ΔH_d, ΔS_d, and ΔG_d, thus indicating a negative correlation between flexibility near the cross-link and folded state stability. Interestingly, Arg^{50} contributes more to protein stability than does Arg^{52}. One might be tempted to attribute this to increased hydrogen bond strength. However, NMR structural and dynamic studies of R50A and R52A (Cai, M., Wen, L., and Krishnamoorthi, R., unpubl.) establish that the R50A mutation also breaks the R52 hydrogen bond, but not vice versa. The decreased ΔC_p values of the R50 and R52 mutants (negative $\Delta\Delta C_p$; Table 1) are consistent with increased hydrophobicity of the folded state (Privalov and Makhatadze 1992; Cai et al. 1996).

Denatured state effect of a cross-link

The previously characterized hydrolysis equilibrium between CMTI-V and CMTI-V* (Cai et al. 1995b) allows one to calculate the effect of a cross-link on the denatured state by means of a four-state thermodynamic cycle comprising native and denatured states of both CMTI-V and CMTI-V* (Fig. 8). The following equation is valid for the thermodynamic cycle:

$$\Delta G^{D}_{hyd} = \Delta G^{N}_{hyd} + \Delta G^{*}_{D} - \Delta G_{D} \quad (2)$$

From the experimental values of 7 and 5 kcal/mole at 25°C for ΔG_D and ΔG^{*}_{D}, respectively (Table T-1 in Electronic Supplemental Material) and a value of −1.3 kcal/mole determined earlier for ΔG^{N}_{hyd} at 25°C (Cai et al. 1995b), we calculate ΔG^{D}_{hyd} at 25°C to be -3.3 kcal/mole. In comparison, native disulfide bond removal in C3S/C48S is accompanied by a free energy change ($\Delta\Delta G_d^{25°C}$) of −4 kcal/mole (Table T-1 in Electronic Supplemental Material). The thermodynamic quantity, $T\Delta S^{d}_{hyd}$, measures the effect of opening the loop formed by the Cys^3-Cys^{48} bridge in the *denatured* state, a quantity more directly related to the theoretical development of the chain-entropy model (Lin et al. 1984). It is calculated as,

$$T\Delta S^{D}_{hyd} = T\Delta S^{N}_{hyd} + T\Delta S^{*}_{D} - T\Delta S_{D} \quad (3)$$

Using the denaturation data obtained for CMTI-V and CMTI-V* (Table 2) and a value of +3.2 kcal/mole for $T\Delta S^{N}_{hyd}$ at 50°C, as calculated from the experimental values (Cai et al. 1995b), we estimate a value of about −1 kcal/mole at 50°C for $T\Delta S^{D}_{hyd}$, which is associated with the opening of the 46-residue loop formed by the Cys^3-Cys^{48} bridge (see Fig. 1). In contrast, the chain-entropy model predicts a value of +4.4 kcal/mole at 50°C, as given by Equation 1.

ΔH^{D}_{hyd} is estimated to be about −5 kcal/mole at 50°C, using a value of +1.6 kcal/mole for ΔH^{N}_{hyd} (Cai et al. 1995b) in the thermodynamic cycle (Fig. 8). Obviously, water-protein interactions play a significant role. Indeed, an enthalpy-entropy compensation, which is generally attributed to solvent-protein interactions (Dunitz 1995), is observed for CMTI-V and the variants (Fig. S-3 in Electronic Supplemental Material). Similar observations have been made with disulfide mutants of barnase (Johnson et al. 1997). Previous studies of engineered disulfide mutants (Matsumura and Matthews 1991; Hinck et al. 1996) have used the reduced form as the unlinked form and evaluated the native state effects on the assumption that energetic effects on the denatured state could be calculated from the chain entropy model. Use of CMTI-V* as another unlinked form of CMTI-V eliminates the need for such an assumption and allows estimation of both native and denatured state effects of a cross-link.

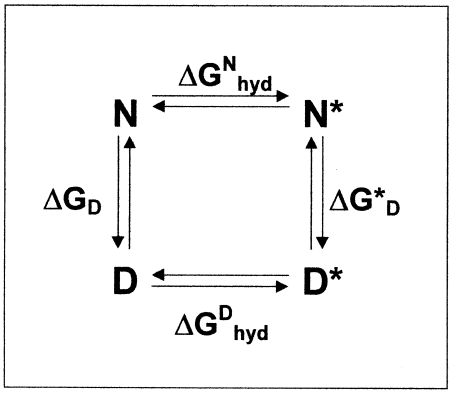

Fig. 8. A four-state thermodynamic cycle consisting of native (N) and denatured (D) states of CMTI-V and CMTI-V*. CMTI-V has a 46-residue loop enclosed by the Cys^3-Cys^{48} bridge. CMTI-V* represents a loop-opened form obtained by specific hydrolysis of the Lys^{44}-Asp^{45} peptide bond. ΔG^{D}_{hyd} and other thermodynamic parameters, related directly to the chain-entropy model, are calculated from the corresponding quantities determined experimentally for the other three processes in the cycle.

Conclusions

The present study of CMTI-V and designed mutants leads to the following conclusions: (1) Removal of a natural disulfide bond destabilizes *both* native and denatured states of a protein, and loss of stability occurs because of a greater native state effect. In comparison, hydrogen bonds seem to affect mainly the native state, and the stabilizing effects of these are less pronounced; (2) An engineered disulfide bond stabilizes *both* native and denatured states. However, greater stabilization of the native state leads to enhanced stability, and that of the denatured state diminished stability; (3) The stabilizing effect of a disulfide bond is because of both enthalpic and entropic contributions, which are modulated by, among others, the following: hydration (or hydrophobicity) of native and denatured states; flexibility in the native state; and residual structure in the denatured state; (4) Mutations that increase flexibility and hydrophobicity of the native state result in destabilization; and (5) The current theoretical models are inadequate in that these do not take into account native structure perturbations causing changes in hydrophobicity, and either neglect or overestimate entropy change caused by hydration of the denatured state.

Materials and methods

Proteins

Recombinant CMTI-V and its mutants were produced by genetic engineering methods, as described previously (Wen et al. 1993).

Mutations were confirmed by DNA sequencing. The proteins were purified using a modified procedure of Wen et al. (1993): the pH of the cell-free extract was adjusted to 3.5, and precipitated impurities were removed by centrifugation. The sample was further purified by ultrafiltration, followed by reverse-phase HPLC, and characterized by trypsin-inhibition assay and sodium dodecyl sulfate-polyacrylamide gel electrophoresis (SDS-PAGE). No covalent dimers or other oligomers were detected with SDS-PAGE under nonreducing conditions, thus excluding formation of intermolecular disulfide bonds. The mutants all inhibited trypsin, albeit at reduced levels (Fig. S-2 in Electronic Supplemental Material), thus implying the presence of a mainly undistorted binding loop. CMTI-V* was prepared by specific hydrolysis of the Lys^{44}-Asp^{45} peptide bond with trypsin, as described previously (Cai et al. 1995b). Freeze-dried protein samples of 1 mg were re-suspended in 1.5 ml 0.1 M glycine buffer at various pH values (2.0, 2.5, 3.0, 3.5). Protein samples were dialyzed twice against 800 ml of the same buffer for a minimum of 10 hr, then centrifuged at 20,000 g. The concentration of the protein in the supernatant was determined from the absorbance at 280 nm using calculated values of molar extinction coefficients (Gill and von Hippel 1989). Corrections because of light scattering were introduced by determining correction parameters at 360 nm and extrapolating these parameters to 280 nm. The corrected absorbance at 280 nm was calculated using the equation:

$$A^*_{280} = A_{280} - A_{360^*}\,(360/280)^4$$

in which A_{280} and A_{360} are the absorbances at 280 and 360 nm.

Reverse-phase HPLC

Retention times of CMTI-V and mutants were determined with a Varian HPLC instrument (Model 2510) with a Varian C-18 column (Fig. S-4 in Electronic Supplemental Material). The eluent consisted of 0.1% (v/v) trifluoroacetic acid in water (solvent A) and 0.1% (v/v) trifluoroacetic acid in acetonitrile (solvent B), pH 2.0. The composition of the eluent was changed by increasing the amount of solvent B in the mixture at a constant rate from 20% to 40% during a 30-min period. The flow rate was maintained at 2 ml/min. The same batch of eluents was used for all the proteins studied.

Determination of total protein sulfhydryl content

The colorimetric method using the Ellman reagent, 5,5′-dithiobis(2-nitrobenzoic acid (DTNB; Habeeb 1975), was used with some modifications. The Ellman reagent was prepared by dissolving 40mg DTNB in 10ml 0.1M sodium phosphate buffer, pH 8.0.

100 μl of 0.05 mM protein (in 0.1 M glycine buffer, pH 2.5) was added to 1 ml 0.1 M sodium phosphate buffer, pH 8.0 (1% SDS, 0.5mg/ml EDTA), followed by 40 μl DTNB stock solution. Color developed over a 15-min interval. The reaction of the protein with DTNB was monitored by recording the spectrum from 360 to 500 nm. The molar concentration of 2-nitro-5-thiobenzoate anion produced in the reaction, and, hence, the molar concentration of reduced sulfhydryl groups in the protein was quantified at 412 nm using a molar absorptivity of 13,600 $M^{-1}cm^{-1}$, following subtraction of the reagent blank. Yeast 3-Phosphoglyceric phosphokinase (Sigma) served as a positive control having one unpaired cysteine. Neither the wild-type CMTI-V nor the mutants had detectable free thiols.

CD measurements

CD spectra were obtained using a Jasco J-720 spectropolarimeter equipped with a water bath. Samples were placed in a 0.01-cm path length cuvette. An average spectrum was calculated from 16 scans recorded for each sample in the 190–250 nm range with a scan speed of 20 nm/min at 25°C. For those variants that were completely unfolded above 80°C, additional spectra were recorded at 85°C.

DSC measurements

DSC measurements were performed using a MicroCal VP-DSC calorimeter. Data were collected under 30 psi pressure using a 60°C/hr scan rate in the 10–115°C range. Solutions were degassed for 10 min before the run. The dialyzate buffer was used to obtain a baseline scan, which was subtracted from protein scans. To check reversibility, at least two scans each were collected for the buffer and proteins used (Fig. S-1 in Electronic Supplemental Material).

DSC data were analyzed using the software, Origin (version 5.0; MicroCal), assuming a two-state mechanism for the thermal denaturation of CMTI-V and mutants. The validity of the assumption was corroborated by the excellent fit of the theoretical two-state curve to the experimental data (Fig. S-5 in Electronic Supplemental Material). The enthalpy of unfolding (ΔH_m) was calculated as the area under the transition peak using the progressive baseline option. ΔS_m, $\Delta H_d(T)$, $\Delta S_d(T)$ and $\Delta G_d(T)$ were calculated using equations (4) – (6):

$$\Delta S_m = \Delta H_m/T_m \tag{4}$$

$$\Delta H_d(T) = \Delta H_m + \Delta C_p(T - T_m) \tag{5}$$

$$\Delta S_d(T) = \Delta S_m + \Delta C_p \ln (T/T_m) \tag{6}$$

$$\Delta G_d(T) = \Delta H_m\,(1 - T/T_m) + \Delta C_p\,[(T - T_m) - T \ln (T/T_m)] \tag{7}$$

The heat capacity changes, ΔC_p, were determined directly from the DSC curves after subtracting the buffer line and normalizing the data, using the step-at-half-peak option. Another way to determine ΔC_p is to measure ΔH_m at different melting temperatures. This is generally achieved by changing the pH of the protein solution. When ΔH_m is plotted as a function of T_m, the slope of the best linear fit to the data gives ΔC_p.

ΔC_p is related to change in water-exposed hydrophobic surface area (Privalov and Makhatadze 1990, 1992), and it is possible that ΔC_p itself is pH-dependent (Mccrary et al. 1998). Experimental data from 20 proteins reveal that ΔC_p decreases with increasing temperature (Makhatadze and Privalov 1995). Indeed, measurements at different pH values revealed a consistent decrease of ΔC_p for CMTI-V and C3S/C48S with increasing melting temperature (Table T-2 in Electronic Supplemental Material). Also, the magnitude of change in melting temperature caused by pH variation was rather small for CMTI-V and its mutants—only 13°C when pH was changed from 2.0 to 3.5 for the wild type, and even less for the mutants. The error in the calculation of ΔH_m together with the error caused by the small temperature range caused an even larger error in the ΔC_p value determined from the ΔH_m versus T_m plot. Therefore, ΔC_p values, as reported in Table 1, were directly measured from the DSC curves.

Electronic supplemental material

Supplemental material includes five figures showing reversibility of DSC scans in the pH range 2.5–3.5, theoretical fits corresponding to the two-state model of reversible thermal unfolding, trypsin-inhibition assays, enthalpy-entropy compensation, and reverse phase HPLC traces, and two tables containing thermodynamic parameters of denaturation at 25°C and variation of ΔC_p with T_m for CMTI-V and mutants.

Acknowledgments

We thank YuXi Gong and Li Zheng for technical assistance. This work was supported in part by grants from the National Institutes of Health (HL-40789) and American Heart Association, Kansas Affiliate. R.K. was supported by an NIH Research Career Development Award (HL-03131; 1994–99). This is contribution 01-198-J from the Kansas Agriculture Experiment Station.

The publication costs of this article were defrayed in part by payment of page charges. This article must therefore be hereby marked "advertisement" in accordance with 18 USC section 1734 solely to indicate this fact.

References

Balbach, J., Seip, S., Kessler, H., Scharf, M., Kashani-Poor, N., and Engels, J.W. 1998. Structure and dynamic properties of the single disulfide-deficient a-amylase inhibitor [C45A/C73A] tendamistat: An NMR study. *Proteins* **33:** 285–294.

Betz, S.F. 1993. Disulfide bonds and the stability of globular proteins. *Protein Sci.* **2:** 1551–1558.

Betz, S.F., Marmorino, J.L., Saunders, A.J., Doyle, D.F., Young, G.B., and Pielak, G.J. 1996. Unusual effects of an engineered disulfide on global and local protein stability. *Biochemistry* **35:** 7422–7428.

Betz, S.F. and Pielak, G.J. 1992. Introduction of a disulfide bond into cytochrome-*c* stabilizes a compact denatured state. *Biochemistry* **31:** 12337–12344.

Bonander, N., Leckner, J., Guo, H., Karlsson, B.G., and Sjolin, L. 2000. Crystal structure of the disulfide bond-deficient azurin mutant C3A/C26A: How important is the S-S bond for folding and stability? *Eur. J. Biochem.* **267:** 4511–4519.

Buck, M., Schwalbe, H., and Dobson, C.M. 1996. Main-chain dynamics of a partially folded protein: ^{15}N NMR relaxation measurements of hen egg white lysozyme denatured in trifluoroethanol. *J. Mol. Biol.* **257:** 669–683.

Byrne, M.P., Manuel, R.L., Lowe, L.G., and Stites, W.E. 1995. Energetic contribution of side chain hydrogen bonding to the stability of staphylococcal nuclease. *Biochemistry* **34:** 13949–13960.

Cai, M., Gong, Y., Kao, J.L.F., and Krishnamoorthi, R. 1995a. Three-dimensional solution structure of *Cucurbita maxima* trypsin inhibitor-V determined by NMR spectroscopy. *Biochemistry* **34:** 5201–5211.

Cai, M., Gong, Y., Prakash, O., and Krishnamoorthi, R. 1995b. Reactive-site hydrolyzed *Cucurbita maxima* trypsin inhibitor-V: Function, thermodynamic stability, and NMR solution structure. *Biochemistry* **34:** 12087–12094.

Cai, M., Huang, Y., Prakash, O., Wen, L., Dunkelbarger, S.P., Huang, J.K., Liu, J., and Krishnamoorthi, R. 1996. Differential modulation of binding loop flexibility and stability by Arg^{50} and Arg^{52} in *Cucurbita maxima* trypsin inhibitor-V deduced by trypsin-catalyzed hydrolysis and NMR spectroscopy. *Biochemistry* **35:** 4784–4794.

Clarke, J. and Fersht, A.R. 1993. Engineered disulfide bonds as probes of the folding pathway of barnase: Increasing the stability of proteins against the rate of denaturation. *Biochemistry* **32:** 4322–4329.

Clarke, J., Henrick, K., and Fersht, A.R. 1995. Disulfide mutants of barnase. I: Changes in stability and structure assessed by biophysical methods and X-ray crystallography. *J. Mol. Biol.* **253:** 493–504.

Cooper, A., Eyles, S.J., Radford, S.E., and Dobson, C.M. 1992. Thermodynamic consequences of the removal of a disulphide bridge from hen lysozyme. *J. Mol. Biol.* **225:** 939–943.

Creighton, T.E. 1993. *Proteins: Structures and molecular properties,* 2nd ed., pp. 419–429. Freeman. New York.

Darby, N. and Creighton, T.E. 1995. Disulfide bonds in protein folding and stability. *Methods Mol. Biol.* **40:** 219–252.

Dill, K.A. 1990. Dominant forces in protein folding. *Biochemistry* **29:** 7133–7155.

Doig, A.J. and Williams, D.H. 1991. Is the hydrophobic effect stabilizing or destabilizing in proteins: The contribution of disulphide bonds to protein stability. *J. Mol. Biol.* **217:** 389–398.

Dunitz, J.D. 1995. Win some, lose some: Enthalpy-entropy compensation in weak intermolecular interactions. *Chem. Biol.* **2:** 709–712.

Eigenbrot, C., Randal, M., and Kossiakoff, A.A. 1990. Structural effects induced by removal of a disulfide-bridge: The X-ray structure of the C30A/C51A mutant of basic pancreatic trypsin inhibitor at 1.6 A. *Protein Eng.* **3:** 591–598.

Flory, P.J. 1956. Theory of elastic mechanisms in fibrous proteins. *J. Am. Chem. Soc.* **78:** 5222–5235.

Futami, J., Tada, H., Seno, M., Ishikami, S., and Yamada, H. 2000. Stabilization of human RNase 1 by introduction of a disulfide bond between residues 4 and 118. *J. Biochem. (Tokyo)* **128:** 245–250.

Gill, S.C. and von Hippel, P.H. 1989. Calculation of protein extinction coefficients from amino acid sequence data. *Analyt. Biochem.* **182:** 319–326.

Goldenberg, D.P. and Creighton, T.E. 1983. Circular and circularly permuted forms of bovine pancreatic trypsin inhibitor. *J. Mol. Biol.* **165:** 407–413.

Habeeb, A.F.S.A. 1975. Reaction of protein sulfhydryl groups with Ellman's reagent. *Methods Enzymol.* **25:** 457–464.

Harper, J.D., and Lansbury, P.T., Jr. 1997. Models of amyloid seeding in Alzheimer's disease and scrapie: mechanistic truths and physiological consequences of the time-dependent solubility of amyloid proteins. *Annu. Rev. Biochem.* **66:** 385–407.

Hinck, A.P., Truckses, D.M., and Markley, J.L. 1996. Engineered disulfide bonds in staphylococcal nuclease: Effects on the stability and conformation of the folded protein. *Biochemistry* **35:** 10328–10338.

Horwich, A.L., and Weissman, J.S. 1997. Deadly conformations—Protein misfolding in prion disease. *Cell* **89:** 499–510.

Ikeguchi, M., Sugai, S., Fujino, M., Sugawara, T., and Kuwajima, K. 1992. Contribution of the 6–120 disulfide bond of a-lactalbumin to the stabilities of its native and molten globule states. *Biochemistry* **31:** 12695–12700.

Inaka, K., Taniyama, Y., Kikuchi, M., Morikawa, K., and Matsushima, M. 1991. The crystal structure of a mutant human lysozyme C77/95A with increased secretion efficiency in yeast. *J. Biol. Chem.* **266:** 12599–12603.

Johnson, C.M., Oliveberg, M., Clarke, J., and Fersht, A.R. 1997. Thermodynamics of denaturation of mutants of barnase with disulfide crosslinks. *J. Mol. Biol.* **268:** 198–208.

Katz, B. and Kossiakoff, A.A. 1990. Crystal structures of subtilisin BPN′ variants containing disulfide bonds and cavities: Concerted structural rearrangements induced by mutagenesis. *Proteins:Struct. Funct. Genet.* **7:** 343–357.

Katz, B.A. and Kossiakoff, A. 1986. The crystallographically determined structures of atypical strained disulfides engineered into subtilisin. *J. Biol. Chem.* **261:** 15480–15485.

Kelly, J.W. 1996. Alternative conformations of amyloidogenic proteins govern their behavior. *Curr. Opin. Struct. Biol.* **6:** 11–17.

Klink, T.A., Woycechowsky, K.J., Taylor, K.M., and Raines, R.T. 2000. Contribution of disulfide bonds to the conformational stability and catalytic activity of ribonuclease A. *Eur. J. Biochem.* **267:** 566–572.

Krishnamoorthi, R., Gong, Y., and Richardson, M. 1990. A new protein inhibitor of trypsin and activated Hageman factor from pumpkin (*Cucurbita maxima*) seeds. *FEBS Lett.* **273:** 163–167.

Kuroki, R., Inaka, K., Taniyama, Y., Kidokoro, S., Matsushima, M., Kikuchi, M., and Yutani, K. 1992. Enthalpic destabilization of a mutant human lysozyme lacking a disulfide bridge between cysteine-77 and cysteine-95. *Biochemistry* **31:** 8323–8328.

Lin, S.H., Konishi, Y., Denton, M.E., and Scheraga, H.A. 1984. Influence of an extrinsic cross-link on the folding pathway of ribonuclease A. Conformational and thermodynamic analysis of cross- linked (lysine7-lysine41)-ribonuclease a. *Biochemistry* **23:** 5504–5512.

Liu, J., Prakash, O., Cai, M., Gong, Y., Huang, Y., Wen, L., Wen, J.J., Huang, J.K., and Krishnamoorthi, R. 1996. Solution structure and backbone dynamics of recombinant *Cucurbita maxima* trypsin inhibitor-V determined by NMR spectroscopy. *Biochemistry* **35:** 1516–1524.

Makhatadze, G.I., and Privalov, P.L. 1995. Energetics of protein structure. *Adv. Protein Chem.* **47:** 307–425.

Matsumura, M. and Matthews, B.W. 1991. Stabilization of functional proteins by introduction of multiple disulfide bonds. *Methods Enzymol.* **202:** 336–356.

Mccrary, B.S., Bedell, J., Edmondson, S.P., and Shriver, J.W. 1998. Linkage of protonation and anion binding to the folding of Sac7d. *J. Mol. Biol.* **276:** 203–224.

Nosoh, Y. and Sekiguchi, T. 1991. *Protein stability and stabilization through protein engineering,* 1st ed., pp. 79–196. Ellis Horwood Limited. Chichester, U.K.

Pace, C.N., Grimsley, G.R., Thomson, J.A., and Barnett, B.J. 1988. Conformational stability and activity of ribonuclease T1 with zero, one, and two intact disulfide bonds. *J. Biol. Chem.* **263:** 11820–11825.

Pakula, A.A. and Sauer, R.T. 1990. Reverse hydrophobic effects relieved by amino-acid substitutions at a protein surface. *Nature* **344:** 363–364.

Pantoliano, M.W., Ladner, R.C., Bryan, P.N., Rollence, M.L., Wood, J.F., and Poulos, T.L. 1987. Protein engineering of subtilisin BPN′: Enhanced stabilization through the introduction of two cysteines to form a disulfide bond. *Biochemistry* **26:** 2077–2082.

Pjura, P.E., Matsumura, M., Wozniak, J.A., and Matthews, B.W. 1990. Structure of a thermostable disulfide-bridge mutant of phage T4 lysozyme shows that an engineered cross-link in a flexible region does not increase the rigidity of the folded protein. *Biochemistry* **29:** 2592–2598.

Poland, D.C. and Scheraga, H.A. 1965. Statistical mechanics of non-covalent bonds in polyamino acids: VIII. Covalent loops in proteins. *Biopolymers* **3:** 379–399.

Privalov, P.L. and Makhatadze, G.I. 1990. Heat capacity of proteins. II. Partial molar heat capacity of the unfolded polypeptide chain of proteins: protein unfolding effect. *J. Mol. Biol.* **213:** 385–391.

Privalov, P.L. and Makhatadze, G.I. 1992. Contribution of hydration and noncovalent interactions to the heat capacity effect on protein unfolding. *J. Mol. Biol.* **224:** 715–723.

Privalov, P.L., Tiktopulo, E.I., Venyaminov, S.Y., Griko, Y.V., Makhatadze, G.I., and Khechinashvili, N.N. 1989. Heat capacity and conformation of proteins in the denatured state. *J. Mol. Biol.* **205:** 737–750.

Qu, B.H., Strickland, E., and Thomas, P.J. 1997. Cystic fibrosis: A disease of altered protein folding. *J. Bioenerg. Biomembr.* **29:** 483–490.

Richards, F.M. and Lim, W.A. 1994. An analysis of packing in the protein folding problem. *Q. Rev. Biophys.* **26:** 423–498.

Sauer, R.T., Hehir, K., Stearman, R.S., Weiss, M.A., Jeitler-Nilsson, A., Suchanek, E.G., and Pabo, C.O. 1986. An engineered intersubunit disulfide enhances the stability and DNA binding of the N-terminal domain of lambda repressor. *Biochemistry* **25:** 5992–5998.

Schwartz, H., Hinz, H., Mehlich, A., Tschesche, H., and Wenzel, H.R. 1987. Stability studies on derivatives of the bovine pancreatic trypsin inhibitor. *Biochemistry* **26:** 3544–3551.

Schwehm, J.M., Kristyanne, E.S., Biggers, C.C., and Stites, W.E. 1998. Stability effects of increasing the hydrophobicity of solvent-exposed side chains in staphylococcal nuclease. *Biochemistry* **37:** 6939–6948.

Shortle, D. 1996. The denatured state (the other half of the folding equation) and its role in protein stabillity. *FASEB J.* **10:** 27–34.

Takagi, H., Takahashi, T., Momose, H., Inouye, M., Maeda, Y., Matsuzawa, H., and Ohta, T. 1990. Enhancement of the thermostability of subtilisin E by introduction of a disulfide bond engineered on the basis of structural comparison with a thermophilic serine protease. *J. Biol. Chem.* **265:** 6874–6878.

Takano, K., Yamagata, Y., Kubota, M., Funahashi, J., Fujii, S., and Yutani, K. 1999. Contribution of hydrogen bonds to the conformational stability of human lysozyme: calorimetry and X-ray analysis of six Ser – Ala mutants. *Biochemistry* **38:** 6623–6629.

Takano, K., Yamagata, Y., and Yutani, K. 1998. A general rule for the relationship between hydrophobic effect and conformational stability of a protein: Stability and structure of a series of hydrophobic mutants of human lysozyme. *J. Mol. Biol.* **280:** 749–761.

Thornton, J.M. 1981. Disulfide bridges in globular proteins. *J. Mol. Biol.* **151:** 261–287.

Tidor, B., and Karplus, M. 1993. The contribution of cross-links to protein stability: A normal mode analysis of the configurational entropy of the native state. *Proteins:Struct. Funct. Genet.* **15:** 71–79.

Ueda, T., Yamada, H., Hirata, M., and Imoto, T. 1985. An intramolecular cross-linkage of lysozyme. Formation of cross-links between lysine-1 and histidine-15 with bis(bromoacetamide)derivatives by a two-state reaction procedure and properties of the resulting derivatives. *Biochemistry* **24:** 6316–6322.

Villafranca, J.E., Howell, E.E., Oatley, S.J., Xuong, N.H., and Kraut, J. 1987. An engineered disulfide bond in dihydrofolate reductase. *Biochemistry* **26:** 2182–2189.

Vogl, T., Brengelmann, R., Hinz, H.J., Scharf, M., Lotzbeyer, M., and Engels, J.W. 1995. Mechanism of protein stabilization by disulfide bridges: Calorimetric unfolding studies on disulfide-deficient mutants of the a-amylase inhibitor tendamistat. *J. Mol. Biol.* **254:** 481–496.

Vogt, G., Woell, S., and Argos, P. 1997. Protein thermal stability, hydrogen bonds, and ion pairs. *J. Mol. Biol.* **269:** 631–643.

Wang, Y. and Shortle, D. 1997. Residual helical and turn structure in the denatured state of staphylococcal nuclease: Analysis of peptide fragments. *Fold. Des.* **2:** 93–100.

Wells, J.A. and Powers, D.B. 1986. In vivo formation and stability of engineered disulfide bonds in subtilisin. *J. Biol. Chem.* **261:** 6564–6570.

Wen, L., Kim, S.S., Tinn, T.T., Huang, J.K., Krishnamoorthi, R., Gong, Y., Lwin, Y.N., and Kyin, S. 1993. Chemical synthesis, molecular cloning, overexpression, and site-directed mutagenesis of the gene coding for pumpkin (*Curcubita maxima*) trypsin inhibitor, CMTI-V. *Protein Express. Purif.* **4:** 215–222.

Wong, K.B., Clarke, J., Bond, C.J., Neira, J.L., Freund, S.M., Fersht, A.R., and Daggett, V. 2000. Towards a complete description of the structural and dynamic properties of the denatured state of barnase and the role of residual structure in folding. *J. Mol. Biol.* **296:** 1257–1282.

Woody, R.W. 1995. Circular dichroism. *Methods Enzymol.* **246:** 34–71.

Zhang, T., Bertelsen, E., and Alber, T. 1994. Entropic effects of disulphide bonds on protein stability. *Nature Struct. Biol.* **1:** 434–438.